Computational Analysis of the Membrane Association of Group IIA Secreted Phospholipases A2: A Differential Role for Electrostatics†

Karthikeyan Diraviyam and Diana Murray*

Department of Microbiology and Immunology and the Institute for Computational Biomedicine, Weill Medical College of Cornell University, New York, New York 10021

Received September 16, 2005; Revised Manuscript Received December 24, 2005

ABSTRACT: Secreted phospholipases A2 (sPLA2's) are enzymes that hydrolyze glycerophospholipids at the sn-2 position, which leads to the production of lipid mediators of many cellular processes. These interfacial enzymes are regulated by their lipid specificity at two levels: membrane binding and substrate recognition. Different sPLA2's utilize different combinations of electrostatic and hydrophobic interactions to adsorb to membrane surfaces, which results in the wide range of membrane binding behaviors observed. Here, the finite difference Poisson Boltzmann (FDPB) method is used to quantitatively analyze the contribution of electrostatic interactions to the membrane association of two highly basic group II sPLA2's: *Agkistrodon piscivorus piscivorus* (AppD49) sPLA2 and nonpancreatic human group IIA (hGIIA) sPLA2. The calculations predict how membrane binding is affected by ionic strength, membrane composition, substitutions of residues in the enzymes, and the presence of calcium in the active site. In addition, the results provide molecular models for the membrane-associated forms of the enzymes. Furthermore, these models account for (1) changes in orientation and protonation state of both the native and charge reversal forms of the enzymes at the membrane surface and (2) the effect of protein/vesicle aggregation, as observed for hGIIA sPLA2. Importantly, the modeling quantitatively describes the complex membrane binding behaviors of these interfacial enzymes in terms of simple physical forces and provides structural information that is difficult to obtain experimentally. The computational analysis shows that nonspecific electrostatic interactions not only play a major role in recruiting these enzymes to membrane surfaces but also orient the enzymes for productive catalysis at the membrane interface.

The reversible binding of proteins to membrane surfaces is critical to many biological processes and is often accomplished through lipid-interacting protein domains. The membrane association of many peripheral membrane proteins has been shown to be mediated, at least in part, by electrostatic and hydrophobic interactions (*1*−*13*). Secreted phospholipases A2 (sPLA2's)[1] are generally recruited to membrane surfaces through a combination of nonspecific electrostatic and hydrophobic interactions, the balance of which can be quite different for different sPLA2 groups (*12*). Dissecting the physical interactions involved and describing the molecular basis of these protein−membrane interactions are crucial to both a unified description and a more detailed understanding of the individual functions and the regulation of these proteins.

sPLA2's have long served as a model family for the study of peripheral membrane association. They have a broad species distribution: they were originally discovered in porcine pancreatic fluid and snake venoms and were subsequently detected in the venoms and pancreatic fluids from a variety of animals (*14*−*17*). More recently, the family has been expanded to include mammalian nonpancreatic sPLA2's, and currently, 10 distinct forms of mammalian sPLA2's are recognized (*14*). sPLA2's are interfacially activated enzymes. They catalyze the hydrolysis of glycerophospholipids at the *sn*-2 ester bond and are clinically important; the products of their catalytic activities, lysophospholipid, and free fatty acids, such as arachidonic acid, have many downstream roles. For example, lysophospholipid is important in cell signaling and phospholipid remodeling, and arachadonic acid can function both as a second messenger and as the precursor of eicosanoids, which are potent mediators of inflammation (*18*, *19*).

sPLA2's have a number of common characteristics, low molecular mass (∼14 kDa), a well-conserved compact three-dimensional structure, which is stabilized by several (5−8) disulfide bonds, and a similar calcium-dependent catalytic mechanism (*20*, *21*). However, there is significant diversity in their membrane binding behaviors. Membrane adsorption and substrate binding have been shown to be separable as two distinct mechanistic steps, and consequently, the physiological functions of sPLA2's are regulated, primarily, by

† Supported by National Institutes of Health Grant GM66147. The calculations were performed on the computers at the Pittsburgh Supercomputing Center (Grant MCB020020P).

* Correponding author. Tel., 212-746-1184; fax, 212-746-8587; e-mail, dim2007@med.cornell.edu.

[1] Abbreviations: sPLA2, secreted phospholipase A2; FDPB, finite difference Poisson Boltzmann; IBS, interfacial binding surface; AppD49 sPLA2, phospholipase A2 from *Agkistrodon piscivorus piscivorus*; hGIIA sPLA2, phospholipase A2 from nonpancreatic human Group IIA.; ΔG_{el}, generally, the calculated electrostatic free energy of interaction between a protein and membrane; PC, phosphatidylcholine; PG, phosphatidylglycerol; PS, phosphatidylserine; MCCE, multiconformation continuum electrostatics method; EPR, electron paramagnetic resonance spectroscopy.

10.1021/bi051901t CCC: $33.50
Published on Web 02/03/2006

their membrane binding preferences, and, secondarily, by their active site selectivity (*22*−*24*). Generally, the surface on sPLA2's that surrounds the active site, termed the "interfacial binding site" or "IBS", adsorbs to membrane surfaces and is rich in basic and hydrophobic residues but may also contain acidic and polar residues. It is believed that the residue composition of the IBS determines the membrane binding preference of sPLA2's (*12*).

There is a large body of experimental literature examining the membrane binding properties of sPLA2's (*25*−*27*). In a number of cases, the effect of specific IBS residues on membrane association and enzyme activation has been elucidated. However, details regarding the relative contributions of electrostatic and hydrophobic forces to membrane association are not clear, and there is a lack of consensus on the significance of electrostatics (*12*, *28*−*31*). To this end, we have chosen to analyze two highly basic sPLA's from the IIA subgroup, a snake species *Agkistrodon piscivorus piscivorus* (AppD49) sPLA2 (*32*) and a human nonpancreatic (hGIIA) sPLA2 (*33*), to more fully characterize the role of electrostatic interactions in membrane adsorption in cases in which electrostatics is believed to be a driving force. The structures for both enzymes are known and are illustrated by their Cα backbone traces in Figure 1. While both contain several hydrophobic residues (green) surrounding the active site cleft, the strong positive equipotential profiles (blues meshes) underlie the observations that both enzymes have very high affinity for anionic membranes but negligible affinity for electrically neutral zwitterionic membranes (*31*, *34*).

We used the finite difference Poisson−Boltzmann (FDPB) method (*35*) to quantitatively analyze the electrostatic component of the membrane interaction of the AppD49 and hGIIA sPLA2's. The FDPB method has been successfully applied to a number of biological systems, and the solution of the full (nonlinear) PB equation has been especially useful in characterizing highly charged systems, such as protein/membrane and protein/nucleic acid systems (*36*−*40*). Both AppD49 and hGIIA sPLA2's have been the subjects of extensive experimental analyses. Therefore, there are many results with which to compare our predictions. Importantly, since our theoretical method is based on well-defined physical principles, the connection between computational and experimental data provides meaningful mechanistic insight unobtainable from experiment alone. Although our calculations employ static models of both the protein and membranes, the comparison with experimental data shows that our analysis captures the physical essence of the biomacromolecular interaction. The computational modeling presented describes how electrostatic forces not only drive the membrane association of two highly basic sPLA2's but also productively orient these enzymes at the membrane interface for efficient catalysis.

EXPERIMENTAL PROCEDURES

The electrostatic free energies and potential profiles were obtained from a modified version of the Delphi program (*35*) that solves the nonlinear Poisson−Boltzmann equation for protein−membrane systems (*37*). The solution for this equation is obtained by using the finite difference (FDPB) method, in which the solvent is described in terms of a bulk dielectric constant and a density function for the mobile ions in the mean field approximation, while solutes (here, the enzymes and phospholipid membranes) are described in terms of the coordinates of their constituent atoms as well as their atomic radii and partial charges (*37*).

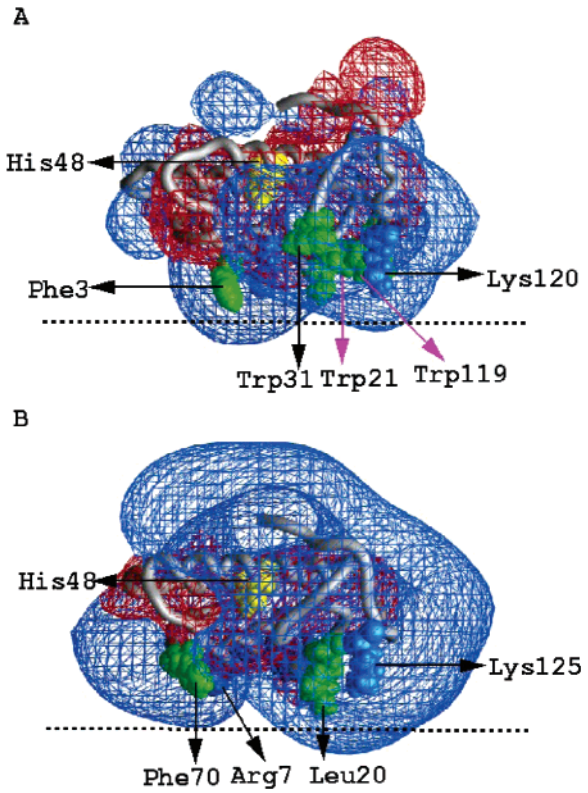

FIGURE 1: Models for the membrane-associated states of two Group IIA sPLA2 enzymes, AppD49 (A) and hGIIA (B) for a PS membrane in 0.1 M KCl. The models are derived from calculations using the FDPB method and orientational sampling (see Experimental Procedures). The proteins are represented by their Cα backbone traces. The atoms of basic and hydrophobic residues on the interfacial binding surfaces (IBS) are represented as blue and green spheres, respectively. Residues discussed in the text are labeled. The membrane surface is represented schematically as a dotted line. Blue (red) meshes represent the +1 kT/e (−1 kT/e) equipotential contours as calculated by the FDPB method for 0.1 M KCl and visualized in GRASP (*51*). Residues were labeled according to the nomenclature followed in refs *33* and *34*. In the case of AppD49, residues labeled 21, 31, 48, 119, and 120 in the figure correspond to residues numbered 20, 30, 47, 109, and 110, respectively, in the PDB file (1VAP). Similarly, for hGIIA, residues labeled 20, 48, 70, and 125 in the figure correspond to residues numbered 19, 47, 63, and 115, respectively, in the PDB file (1POD).

Structural Models. The enzymes AppD49 sPLA2 (PDB identifier 1VAP) and hGIIA sPLA2 (PDB identifier 1POD) were represented by the coordinates of their crystal structures (*34*, *42*). The AppD49 sPLA2 structure was solved in the absence of calcium. Therefore, a calcium ion was placed into its active site by structurally aligning it, using the structure superposition program CE (Combinatorial Extension) (*43*), with a related protein structure that has a calcium ion in its active site cleft (1JIA, a basic sPLA2 from the snake species *Agkistrodon halys pallas*). The two structures superimpose with a root-mean-square deviation (rmsd) of 0.8 Å with a related *Z*-score of 6.7. Once superimposed, the coordinates for the calcium ion from 1JIA were transferred to 1VAP. For both AppD49 and hGIIA sPLA2's, it was assumed that the calcium-free and calcium-bound structures are similar

and differ only by the absence or presence, respectively, of the active site calcium. This is a valid assumption, considering the structural rigidity of sPLA2's (several disulfide bonds) and the fact that the calcium-free and calcium-bound forms of other sPLA2's whose structures were solved are structurally similar. For example, in the case of hGIIA sPLA2, a pair of structures solved with (1POD) and without (1BBC) calcium superimpose with an rmsd of 1.4 Å and a *Z*-score of 6.6. The program CHARMM (*44*) was used to add hydrogen atoms to the heavy atoms and to construct residue-substituted forms of the proteins.

Phospholipid bilayers were built as described previously (*37*, *45*), except for calculations modeling vesicle aggregation (see below). In this study, we considered membranes with the following compositions: 0:1, 3:1, 2:1, 5:1, and 1:0 PC/PS (PC, phosphatidylcholine; PS, phosphatidylserine). As in previous work (*37*−*40*, *45*), we assumed that the bilayer lipids change neither structure nor position upon interaction with the protein (see Discussion for further comments on this point).

Electrostatic Calculations. Each atom of a protein/bilayer system is assigned a radius and partial charge that is located at its "nucleus"; that is, each atom is considered a simple sphere. The protein/membrane model is then mapped onto a three-dimensional lattice of l^3 points, each of which represents a small region of the protein, membrane, or solvent. The charges and radii used for the amino acids were taken from a CHARMM22 parameter set (*44*), and those used for the lipids are the ones described in Peitzsch et al. (*45*) and used in our previous studies. Regions inside the solvent-accessible surfaces of the protein and membrane are assigned a dielectric constant of 2 to account for electronic polarizability, and those outside are assigned a dielectric constant of 80 (*46*). An ion exclusion layer is added to the solutes and extends 2 Å beyond their molecular surfaces. The nonlinear Poisson−Boltzmann equation is solved in the finite difference approximation, and the numerical calculation of the potential is iterated to convergence, which is defined as the point at which the potential changes less than 10^{-4} kT/e between successive iterations (*35*). Electrostatic free energies are obtained from the calculated potentials (*41*), and the electrostatic free energy of interaction is determined as the difference between the electrostatic free energy of a protein in a specific orientation with respect to the membrane surface, $G_{el}(P\cdot M)$, and the electrostatic free energies of the protein, $G_{el}(P)$, and membrane, $G_{el}(M)$, infinitely far apart; that is, taken separately

$$\Delta G_{el} = G_{el}(P\cdot M) - [G_{el}(P) + G_{el}(M)] \qquad (1)$$

Misra and Honig (*47*, *48*) solved the nonlinear Poisson−Boltzmann equation with the FDPB method to calculate the pK_a shift of a titratable group on an antibiotic upon binding to DNA. Their results are in excellent agreement with experimental observations. More recently, we applied a similar scheme to predict the pK_a shifts of glutamates on the IBS of bee venom sPLA2 (bvPLA2) upon membrane association (*39*)

$$\Delta pK_a = [1/(2.3kT)][\Delta G^-_{el} - \Delta G^\circ_{el}] \qquad (2)$$

where ΔG^-_{el} and ΔG°_{el} are calculated as described for eq 1, and ΔG^-_{el} represents the electrostatic free energy of membrane interaction of the enzyme, while ΔG°_{el} represents the electrostatic free energy of membrane interaction of the enzyme with the residue of interest, that is, either a glutamate or a histidine, in its protonated form. The positive/negative pK_a shifts calculated depend on how favorable/unfavorable it is for that residue to be protonated in the presence of the membrane.

All electrostatic free energies (eqs 1 and 2) are calculated for various distances of separation between the van der Waals surfaces of the enzyme and membrane. The protein and membrane are treated as static entities, and only the relative orientation of the protein with respect to the membrane is varied. In cases where it is known or predicted that hydrophobic residues penetrate the membrane interface, the side chains of these residues are removed so that the membrane-docked protein more realistically approximates the enzyme in its membrane-associated state. Removing the side chains of these residues changes the molecular surface of the IBS of the enzyme and places charged residues in closer proximity to the membrane surface (*39*, *40*).

In all FDPB calculations, a sequence of focusing runs (*49*) of increasing resolution was employed to calculate the electrostatic potentials (i.e., 0.375, 0.75, 1.5, 3.0 grid/Å). In the initial calculation, the protein/membrane model encompasses a small percentage of the lattice (∼20%), and the potentials at the boundary points of the lattice are approximately 0; this procedure both ensures that the system is electroneutral and provides initial values for the boundary grid points. Lattice sizes of 289^3 (cubic grid points) were used, and the calculations were performed to final resolutions of 3.0 grid/Å. The precision in the electrostatic free energies of interaction, determined as the difference between the results obtained at the two highest resolution scales, that is, 1.5 grid/Å and 3.0 grid/Å, is ≤0.3 kcal/mol for all calculations, though a precision of 0.1 kcal/mol was more typical. We stress that precision is not the same as accuracy, and that there may be many factors that affect the latter for which we do not account (see Discussion). The precision in the calculated pK_a shifts is ≤0.2 units. The solution pK_a values, for those residues whose pK_a shifts were predicted at the membrane surface based on our electrostatic free energy analysis, were calculated using the multiconformation continuum electrostatics (MCCE) method (*50*). All values calculated with MCCE are compiled in Tables S1 (for AppD49 sPLA2) and S2 (for hGIIA sPLA2) in the Supporting Information. Since the residues we examined are located on the protein surface and largely solvated, most of the solution values are similar to those expected for the isolated amino acids, that is, pK_a (Glu) ∼ 4−5 and pK_a (His) ∼ 6−7. However, several residues are predicted to have solution pK_a values that are significantly different from the isolated pK_a values. For example, some glutamates have very low solution pK_a values. This may be due to the highly basic character of the surface on which these residues are located (Figure 1), which would tend to drive the pK_a's of glutamates in these regions to lower values than those obtained in less electropositive regions. On the other hand, the calculated solution pK_a for the AppD49 K16E substitution is ∼7. When the structure is analyzed, it is observed that the side chain of E16 is partially buried, which would favor the protonated form and a higher pK_a value. However, the native K16 has

a much longer side chain, whose terminus is solvent-exposed. Thus, the calculated solution pK_a for E16 may be an artifact of our modeling of the residue swap. It is noteworthy that MCCE uses the linearized Poisson−Boltzmann equation which may not be appropriate for the highly charged group II sPLA2's considered here. Indeed, the equipotential difference map calculated from linear versus the nonlinear electrostatic calculations for AppD49 sPLA2 suggests significant differences in potential values near the surface of the protein that may affect the calculated solution pK_a values (see Figure S1 in Supporting Information).

Determining the Minimum Electrostatic Free Energy of Interaction between an sPLA2 and the Membrane Surface. As qualitatively illustrated by the potential profiles in Figure 1, favorable values for ΔG_{el}, as determined by eq 1, are expected for a wide range of orientations for both enzymes at the membrane surface. To identify more precisely the minimum electrostatic free-energy orientations of the enzymes at the membrane surface, ΔG_{el} was calculated for orientations sampled about the one which was judged visually to approximate the minimum free-energy orientation based on the potential profile of the enzyme as obtained in GRASP (*51*). The enzyme was rotated in steps of 10° in the *X*- and *Y*-directions (*Z* is normal to the membrane surface). If, after comprehensive sampling, a more favorable orientation, that is, ΔG_{el}, was obtained, this was then taken as the minimum free-energy orientation. Previous work has established that, for peripheral association, both the relative binding free energies and the electrostatic contribution to absolute binding free energies are well-approximated by consideration of the minimum free-energy orientation alone (*37*, *38*, *40*, *52*). In the case of hGIIA sPLA2, because of its contiguous positive potential distribution (Figure 1B), sampling analysis resulted in two equivalent minimum electrostatic free-energy orientations (see Results). Hence, to represent a catalytically active minimum electrostatic free-energy orientation, we used the orientation in which the IBS faces the membrane for most of our calculations. The minimum electrostatic free-energy orientation for AppD49 sPLA2 obtained from orientation sampling analysis (Figure 1A) has its IBS directed toward the membrane and is, thus, predicted to be a catalytically competent orientation.

Calculations for Membrane Aggregation Induced by hGIIA sPLA2. Our goal is to produce an unbiased model for membrane aggregation that does not have the known outcome built into it. Larger 2:1 and 0:1 PC/PS bilayers (340 PS lipids per leaflet) were used than those in the calculations described previously so that multiple sPLA2's may be spatially accommodated at the membrane surfaces. Each hGIIA sPLA2 is oriented on the first bilayer in its minimum electrostatic free-energy orientation as determined previously with its active site facing the membrane surface, in the absence of other sPLA2's. The apposing bilayer is placed parallel to the first but approximately 2 Å away from the van der Waals surface of the opposite surface of the enzyme docked at the surface of the first bilayer; this placement of the second bilayer corresponds to a second minimum electrostatic free-energy orientation for the hGIIA sPLA2 (see Results). To simulate the aggregation behavior, the electrostatic free energies of interaction between the membranes in the presence and absence of enzyme are compared under two conditions, as described in Results. For all configurations, the membranes overlap the imprint of the sPLA2's by at least 20 Å (greater than 2 D lengths in 0.1 M KCl) in order to avoid edge effects. Lattice sizes of up to 401^3 were used, and the calculations were performed to final resolutions of up to 4.0 grids/Å. The electrostatic free energy of aggregation is given as the difference between the electrostatic free energy of the membrane/enzyme/membrane configuration, $G_{el}(M{\cdot}P{\cdot}M)$, and the electrostatic free energy of enzyme prebound to one membrane surface, $G_{el}(M{\cdot}P)$, and a second membrane, $G_{el}(M)$, infinitely separated (analogous to eq 1)

$$\Delta G_{el}(\text{aggregation}) = G_{el}(M{\cdot}P{\cdot}M) - G_{el}(M{\cdot}P) - G_{el}(M) \quad (3)$$

RESULTS

Nonspecific Electrostatic Interactions Facilitate the Adsorption of AppD49 and hGIIA sPLA2's at Membrane Surfaces in Catalytically Productive Orientations. Electrostatic forces play an important role in orienting many peripheral proteins at membrane surfaces (*53*, *54*). One of the first studies to suggest this visually inspected the electrostatic potential profiles for a number of sPLA2's of known structure and predicted that the large positive potential profiles surrounding the active sites should contribute to the adsorption of sPLA2's to anionic membranes (*28*). Here, we test this prediction more quantitatively by predicting the minimum electrostatic free energy orientations of AppD49 and hGIIA sPLA2's using atomic models for the proteins and membranes and the FDPB method. Calculations were performed with mixed zwitterionic/acidic phospholipid bilayers and 0.05−2.0 M KCl as appropriate to the experimental studies. The minimum electrostatic free-energy orientations were obtained by sampling many different orientations of each sPLA2 with respect to the membrane surface and calculating ΔG_{el}, the electrostatic free energy of interaction, as described for eq 1 in Experimental Procedures. The minimum electrostatic free-energy orientations obtained for the AppD49 and hGIIA sPLA2's are shown in Figures 1, panels A and B, respectively. Hydrophobic residues surrounding the active site cleft are colored green, and the blue and red meshes represent positive and negative equipotential contours, respectively. It is apparent that both enzymes are oriented so that their interfacial binding surfaces (IBS) interact with the membrane, that is, in presumably catalytically productive orientations. Hence, the electrostatic characteristics of these proteins are optimally configured to support enzymatic function. Experimental studies have shown that the hydrophobic residues on the IBS penetrate the membrane interface. In the case of AppD49 sPLA2 (Figure 1A), experiments (*55*) show that the fluorescent intensities of residues W21 and W119 (pink arrows in Figure 1A), but not residue W31 (black arrow), are affected by the presence of anionic vesicles, indicating that the former are part of the IBS, as we predict, while the latter is located away from the membrane, also consistent with our prediction. In the case of hGIIA sPLA2 (Figure 1B), we predict a membrane-associated orientation consistent with residue-substitution experiments that have identified the IBS (*31*) as well as the EPR-determined orientation of hGIIA sPLA2 on the surface of an anionic membrane (*56*). Additional IBS residues that were determined experimentally

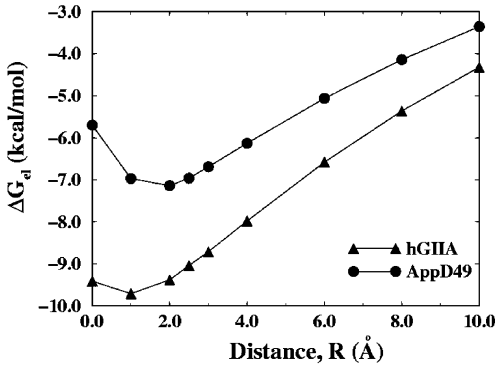

FIGURE 2: Nonspecific electrostatic contribution to the membrane association of Group IIA sPLA2's. The electrostatic free energies of interaction for AppD49 (circles) and hGIIA (triangles) sPLA2's in their minimum free-energy orientations are calculated as a function of the distance between the van der Waals surfaces of the enzymes and a PS membrane in 0.1 M KCl.

and predicted based on our analysis are labeled in Figure 1B. The minimum free-energy orientations depicted in Figure 1 are used throughout this study unless stated otherwise.

Nonspecific Electrostatic Interactions Contribute Significantly to the Membrane Recruitment of AppD49 and hGIIA sPLA2's. Figure 2 shows the electrostatic free energy curves for both enzymes, that is, ΔG_{el} plotted as a function of the minimum distance between the van der Waals surfaces of the enzymes and membrane. Even when the protein is at least 1 D in length (~10 Å for 0.1 M KCl) away from the membrane surface, there is a significant Coulombic attraction to the negatively charged membrane. For both enzymes, the minimum electrostatic free energy of interaction is predicted to occur when both the enzyme and membrane are almost fully solvated; the minimum free-energy orientations depicted in Figure 1 for AppD49 and hGIIA sPLA2's occur at $R =$ 2.0 and 1.5 Å, respectively. In addition, the minimum electrostatic free energy of interaction is ~2.5 kcal/mol more favorable for hGIIA sPLA2 (triangles, Figure 2) than for AppD49 sPLA2 (circles, Figure 2); this is consistent with the fact that the net charge of hGIIA sPLA2 is almost twice as large (+17) as that of AppD49 sPLA2 (+8). However, as seen in Figure 1, the positive charge is spread uniformly over the surface of hGIIA sPLA2, whereas the charge distribution of AppD49 sPLA2 is more polarized and the positive potential is localized to the IBS. It is important to note that at $R = 0$ Å, where there is significant desolvation of both the highly charged protein and membrane, ΔG_{el} is still quite favorable for both enzymes: ΔG_{el} ($R = 0$ Å) ~ −5.5 and −9.5 kcal/mol for AppD49 sPLA2 and hGIIA sPLA2, respectively. This implies that favorable electrostatic interactions contribute significantly not only to the recruitment of the enzymes to membranes (at large R) but also to their final binding free energies when they are in close apposition to the membrane surface (i.e., at $R \sim 0$ Å). Therefore, favorable nonpolar interactions, mediated by the partitioning of hydrophobic residues on the IBS into the membrane interface, should combine with the favorable electrostatic interaction at small R to produce enhanced membrane association.

The basic residues which are responsible for the enzymes' high affinity for anionic membranes also select against neutral membranes. This is illustrated in Figure 3 , panels A and B, which plot the predicted minimum ΔG_{el} for the

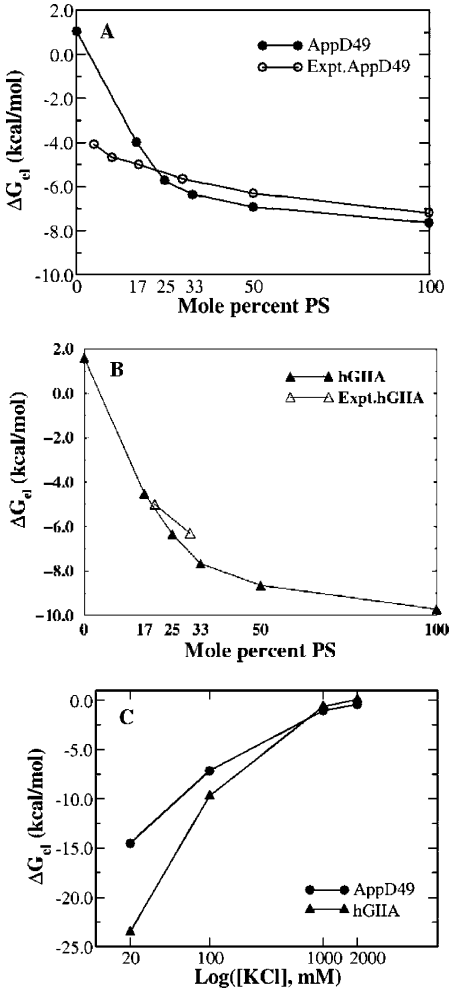

FIGURE 3: Dependence of the nonspecific electrostatic interaction between Group IIA sPLA2's and the membrane surface on mole percent acidic phospholipid (A and B) and ionic strength (C). The electrostatic free energy of interaction of AppD49 (A) and hGIIA (B) sPLA2's decreases as the mole percent acidic lipid in the membrane increases at an ionic strength of 0.05 M KCl without calcium and 0.1 M KCl with calcium, respectively. The closed symbols are the calculated minimum electrostatic free energies, and the open symbols correspond to experimentally derived free-energy values for the respective enzymes (AppD49 sPLA2 (*30*); hGIIA sPLA2 (*29*)). (C) The electrostatic free energy of interaction of AppD49 and hGIIA sPLA2's with a PS membrane surface increases as the salt concentration is increased as seen experimentally (*34*, *56*−*58*).

AppD49 and hGIIA sPLA2's as a function of mole percent PS in the membrane for 0.05 M KCl without calcium and 0.1 M KCl with calcium, respectively, to match the experimental conditions. (For PC membranes, ΔG_{el} calculated at $R = 2$ Å for both enzymes is plotted.) As expected, when there is no acidic lipid in the membrane, there is no favorable electrostatic interaction in this (or any) orientation; in fact, the interaction is repulsive at all distances R between the enzymes and the membrane (data not shown). For example, at $R = 0$ Å, the electrostatic free energy of interaction is about +3.0 and +2.6 kcal/mol for AppD49 and hGIIA, respectively, on a PC membrane. Similarly, for a purely anionic membrane, as stated above, the corresponding values are −5.7 and −9.5 kcal/mol (Figure 2). This suggests that electrostatic repulsion with a PC membrane, but not a membrane containing PS, would likely preclude the proteins from binding the membrane in a catalytically productive

orientation even in the presence of nonpolar contributions.

Experiments show that both AppD49 and hGIIA sPLA2's bind very strongly to membranes containing acidic lipids (*29*, *30*; Figure 3A,B open circles). In the case of AppD49 sPLA2, our predictions underestimate the binding at lipid compositions containing less than 20 mol % acidic lipid; this may be due to the dominance of favorable nonpolar contributions over electrostatic repulsion (see Discussion). Alternatively, experiments show that AppD49 sPLA2 may experience different binding modes as a function of mole percent acidic lipid (*30*). Because of its highly basic nature and problems associated with vesicle aggregation (see below), it is technically difficult to measure the affinity of hGIIA sPLA2 to membranes containing greater than 30 mol % acidic lipid. Our predictions of the relative binding as a function of the mole percent acidic lipid in the membrane are in good agreement with experiments as depicted in Figure 3A,B (compare filled and open symbols); the electrostatic free energy of interaction becomes significantly more favorable as the acidic lipid concentration is increased. For example, experiments show that AppD49 sPLA2 (in 0.05 M KCl) binds 30-fold more strongly to PG (phosphatidylglycerol) membranes than to membranes containing 20 mol % PG (*30*), while hGIIA sPLA2 (in 0.1 M KCl) binds 10-fold more strongly to membranes containing 30 mol % PS versus 20 mol % PS (*29*); our calculations predict the binding is stronger by 45-fold for AppD49 sPLA2 and 12-fold for hGIIA sPLA2, in excellent agreement with these observations.

As seen in Figure 3A,B, the minimum ΔG_{el} is -2.5 and -4.5 kcal/mol for AppD49 sPLA2 and hGIIa sPLA2, respectively, when there is 17 mol % PS in the membrane. The minimum ΔG_{el} decreases further (to -5.8 and -8.0 kcal/mol, respectively) for 33 mol % PS. Therefore, the change in the minimum ΔG_{el} is quite dramatic in a physiological range of acidic lipid, suggesting there is a strong selectivity for negatively charged membrane surfaces. The slope in Figure 3A,B becomes less steep above 33 mol % acidic lipid because there is an increasingly significant unfavorable desolvation of the more negatively charged membrane surfaces by the proteins that is strong enough to compensate for gains in the favorable Coulombic attraction (Mirkovic and Murray, unpublished results).

Experimental studies on both enzymes (*34*, *56*−*58*) have shown that increasing the ionic strength of the solution affects their membrane binding properties as expected for electrostatically driven interactions. In the case of AppD49 sPLA2, the binding to acidic phospholipid vesicles is 500-fold weaker in 1 M KCl than in 0.16 M NaCl. Our calculations predict that the binding decreases ~1000-fold as the ionic strength increases from 0.1 to 1 M KCl, in good agreement with experimental data (Figure 3C). In contrast, there are no direct measurements of the salt dependence of the membrane binding of hGIIA sPLA2. However, Beers et al. (*57*) observe that under conditions of high salt (2 M KCl) the electrostatic contribution to the lipase activity of hGIIA sPLA2 on small unilamellar vesicles is minimal; the absolute specific activity of the native enzyme decreased from 96 to 43 (nmol/min)/μg when the salt was increased from 0.1 to 2 M, while the activity of a residue-substituted variant with a more hydrophobic IBS (V3W) increased from 111 to 251 (nmol/min)/μg. Since these are interfacial enzymes, it is reasonable to assume that a weakened electrostatic interaction accounts for the lower activity of the native enzyme, whereas the activity of V3W increases with salt, which is known to enhance hydrophobic interactions. As seen in Figure 3C, our calculations predict that membrane binding is significantly depressed with increasing ionic strength.

Experimental and structural studies have elucidated the indispensable role of calcium in the catalytic activity of sPLA2's. In addition, experiments (*39*, *59*) suggest that calcium in the active site may increase the membrane binding affinity of AppD49 and bee venom sPLA2's. Attenuated total reflection Fourier transform infrared (ATR-FTIR) spectroscopy was used to determine the effect of calcium on the binding of AppD49 to 20% PG membranes in 0.115 M NaCl. A slight increase in membrane binding was observed with respect to membrane binding in the absence of calcium ($\Delta\Delta G_{el} = -0.3$ kcal/mol). However, the interpretation of these results is not clear, as hydrolysis of lipids was observed when calcium was present. Our predicted $\Delta\Delta G_{el}$ for 17% PS in 0.1 M KCl of -0.6 kcal/mol is consistent with the small experimental observation. Similar experimental studies have not been performed for hGIIA sPLA2, whose inherent basic nature already confounds membrane binding studies. For pure acidic phospholipid membranes in 0.1 M KCl, we predict that the presence of a calcium ion in the active site decreases ΔG_{el} for the AppD49 and hGIIA sPLA2's by 1.6 and 2.5 kcal/mol, respectively. In our previous study on bee venom sPLA2 (bvPLA2; *39*), our calculated $\Delta\Delta G_{el}$ values significantly overestimated the observed effect of calcium as the experiments were not able to tease out the contribution of bound lipid in the active site. Hence, our calculations have value in estimating how calcium alone, in the absence of bound substrate, enhances the electrostatic binding of sPLA2's to membranes containing anionic phospholipids.

Overall, our calculations provide a more detailed description of the nonspecific electrostatic component to the membrane association of the group IIA sPLA2's than is obtainable from experimental analysis both because our calculations can isolate the electrostatic interactions and because the extremely high affinity of these enzymes for anionic membranes renders experimental analysis extremely challenging.

Large pK_a Shifts Are Predicted for Glutamate Residues on the IBS of Membrane-Adsorbed sPLA2's. Many studies on the membrane association of sPLA2's have relied on charge reversal substitutions to discern the effect of basic residues and, hence, electrostatic interactions on membrane adsorption; generally, lysine and arginine residues on the IBS are changed to glutamates (*12*). However, these charge reversal substitutions, that is, the replacement of a basic residue by an acidic residue, could potentially overestimate the contribution of the native basic residue to favorable electrostatic interactions with a negatively charged membrane surface if the acidic residue introduces a charge−charge electrostatic repulsion with the membrane. In other words, if we assume that the desolvation of both the basic residue and its substituted acidic residue is similar, then the apparent contribution of the basic residue will not only be the loss of favorable Coulombic attraction but also an additional quantity, that is, the electrostatic repulsion between the acidic residue and acidic lipids. This situation is not straightforward

Table 1: pK_a Shifts Calculated for the Substituted Glutamates in the IBS of AppD49 sPLA2[a]

enzyme form, residue for which pK_a was calculated	pK_a shift of the mutated residue at the membrane prior penetration		pK_a shift of the mutated residue at the membrane after penetration
	$R = 0.0$ Å	$R = 2.0$ Å	$R = 0.0$ Å
native, E6	2.0	1.5	2.6
engineered, K7E/K10E	2.8	2.1	5.0
engineered, K7E	1.4	1.1	1.8
engineered, K10E	1.9	1.4	3.5
engineered, K11E	0.9	0.7	1.1
engineered, K16E	0.9	0.7	1.1
engineered, K54E	0.1	0.1	0.1

[a] pK_a shifts were calculated using the FDPB method for the orientation in Figure 1A and PS membrane in 0.1 M KCl. The values are calculated as a function of distance, *R*, between the van der Waals surface of the enzyme and membrane. Values in column 4 were calculated with the side chains of hydrophobic residues on the IBS that probably penetrate the membrane interface removed.

Table 2: pK_a Shifts Calculated for the Substituted Glutamates in the IBS of hGIIA sPLA2[a]

enzyme form, residue for which pK_a was calculated	pK_a shift of the mutated residue at the membrane prior penetration		pK_a shift at the membrane after penetration
	$R = 0.0$ Å (no penetration)	$R = 2.0$ Å	$R = 0.0$ Å (assumed penetration)
native, E17	2.2	1.7	~4.0−4.5
R7G/K10G, E17	1.8	1.3	3.5
R7E/K10E/K16E, E17	1.5	1.0	4.5
K74E/K87E/R92E, E74	0.6	0.5	0.7
K7E, E7	1.2	0.9	1.7
native, H6	1.8	1.4	2.3
H6E, E6	2.1	1.6	~3.8−4.1

[a] pK_a shifts were calculated using the FDPB method for the orientation in Figure 1B and a PS membrane in 0.1 M KCl. The values are calculated as a function of distance, *R*, between the van der Waals surface of the enzyme and membrane. Values in column 4 were calculated with the side chain of hydrophobic residues on the IBS that probably penetrate the membrane interface removed.

as there is no direct evidence as to how the protein responds to a charge reversal substitution at the membrane surface. Recent studies (*39*, *60*, *61*) suggest that glutamates on the membrane binding surfaces of peripheral proteins may become protonated and, hence, neutralized at the membrane interface. Thus, charge reversal substitutions may be less perturbing than described above. In addition, the magnitude of the effect is expected to depend on the biophysical character and shape of the IBS on a protein, the amount of acidic lipid in the membrane, and the ionic strength of the solution. Indeed, our previous work on bvPLA2 concluded that there is no universal prescription for dealing with this issue and that each case has to be considered separately (*39*). There is a large amount of data on the effect of charge reversal substitutions on the membrane association of AppD49 and hGIIA sPLA2's, which affords us the opportunity to test the ability of electrostatic theory to explain a wide range of experimental observations (*25*−*27*, *29*−*34*).

The pK_a shifts (ΔpK_a's) of glutamates present on the IBS of both the native and glutamate-substituted forms of AppD49 and hGIIA sPLA2's were calculated for PS membranes in 0.1 M KCl, and the results are listed in Tables 1 and 2, respectively, for each enzyme. To understand the effect of membrane proximity on the pK_a shifts, the calculations were performed under three different conditions: (1) when the distance of closest approach between the van der Waals surfaces of enzyme and membrane is 2 Å, which corresponds approximately to the minimum electrostatic free-energy orientation (see Figure 2), so that both the enzyme and membrane are mostly solvated (column 2); (2) when the distance of closest approach between the van der Waals surfaces of the enzyme and membrane is 0 Å, that is, the surfaces are just touching but no hydrophobic residues are penetrating the interface (column 3); and (3) when the hydrophobic residues on the IBS are assumed to be penetrating the membrane interface (column 4). Since our calculations are based on static representations of the enzymes and membranes, we modeled the third condition by simply removing the side chains from the hydrophobic residues on the IBS of each enzyme, as described in Experimental Procedures, and performing the FDPB calculations with these altered forms; this is meant to approximate the situation of an interfacially associated enzyme, and the predicted pK_a shifts calculated for these forms are, thus, likely the most physiologically representative.

As depicted in Table 1 for AppD49, significant pK_a shifts are predicted for E6 in the native enzyme (row 1) as well as for E7 and E10 for glutamate-substituted forms (rows 3 and 4) under almost all conditions ($1.1 \leq \Delta pK_a \leq 3.5$). As illustrated in Figure 4A, each of these positions are centrally located on the IBS. Not surprisingly, the largest predicted shifts are obtained for condition 3 in which the IBS is closest to the membrane interface (note that ΔpK_a increases consistently from column 2 to 4 in Table 1). Furthermore, Figure 5 (circles) illustrates how ΔpK_a increases dramatically for E6 in native AppD49 sPLA2 with the mole percent acidic lipid in the membrane (assuming condition 3, i.e., column 4 of Table 1). Note, however, that the calculated ΔpK_a is actually negative (−0.8) for electrically neutral (PC) membranes. This is in sharp contrast to our earlier work on the "E5" form of bvPLA2 (bvPLA2-E5, where five basic residues were substituted by glutamates) for which we predict significant positive pK_a shifts for glutamates close to the interface of a PC membrane (*39*). The origin of this effect lies in the dramatic difference in the electrostatic properties of the interfacial binding surfaces of these two enzymes. The overall electronegative character of the IBS of bvPLA2-E5 ensures that it is energetically favorable for the probability of protonation to increase for glutamates close to the interface of a membrane of any composition. In the case of a PC membrane, protonation would serve to decrease the desolvation penalty of the acidic IBS upon membrane adsorption. In contrast, for the IBS of native AppD49 sPLA2, its electropositive character is so strong and its basic residue density is so high (Figures 1A and 4A), that a negatively charged glutamate will help reduce the desolvation upon adsorption to a PC membrane by neutralizing, at least in part, neighboring basic residues. Hence, protonation at the surface of a PC membrane is disfavored. It is only when repulsive charge−charge interactions between the glutamate and acidic lipids become sufficiently strong that the pK_a shift is large and positive, that is, when the mole percent PS is greater than 33 (Figure 5, circles). Relevant to experiments, since

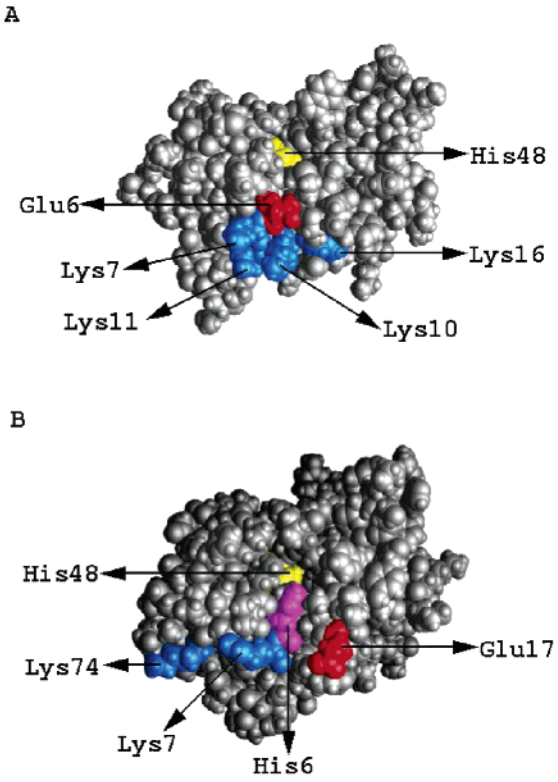

FIGURE 4: Space filling representations of the AppD49 and hGIIA sPLA2 IBS depicting residues whose electrostatic contributions to membrane association have been examined experimentally and, in this study, computationally. AppD49 (A) and hGIIA (B) sPLA2's are oriented with their IBS facing the viewer. The catalytic histidine is colored yellow, and residues for which significant pK_a shifts are predicted (see Tables 1 and 2) are labeled as follows: red represents wild-type glutamates, blue represents basic residues that are substituted by glutamates, and magenta represents the IBS histidine in hGIIA sPLA2.

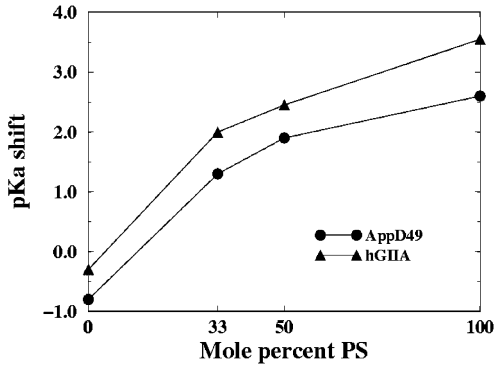

FIGURE 5: Dependence of the pK_a shifts of glutamates on the IBS of native Group II sPLA2's on the mole percent acidic phospholipid in the membrane. The calculated pK_a shifts of Glu6 on AppD49 sPLA2 are denoted by circles, and those for Glu17 on hGIIA sPLA2 are denoted by triangles. In both cases, the pK_a shift increases as the mole percent acidic lipid is increased in the membrane at a fixed ionic strength of 0.1 M KCl.

AppD49 sPLA2 does not bind appreciably to PC membranes, these calculations indicate that, upon membrane adsorption, the desolvation of substituted or native glutamates on the IBS and the strong electrostatic environment due to the negatively charged membrane surface both play significant roles in the upward shifts of the pK_a's of these residues.

As suggested by Figures 1 and 4, there is large desolvation of both the enzyme and membrane when the enzyme is in a catalytically competent membrane-adsorbed orientation. In addition, the electrostatic charge−charge repulsion between an IBS glutamate and the surface of a negatively charged membrane is also large, even though the overall electrostatic attraction between the enzyme and membrane is still quite strong (in Figure 2 (circles), $\Delta G_{el} \sim -6$ kcal/mol at $R = 0$ Å). Based on the predicted ΔpK_a's (Table 1) and the calculated solution pK_a's (as obtained from MCCE; see Experimental Procedures and Table S1, Supporting Information), we predict that in the final membrane-adsorbed state (for 100 mol % PS and 0.1 M KCl), the pK_a of E6 is 3.3 + 2.6 = 5.9, while the pK_a's of E7 and E10 in the substituted enzymes are 3.4 + 1.8 ∼ 5.2 and 3.7 + 3.5 = 7.2, respectively, where the first number in the sum is the solution pK_a and the second is the calculated pK_a shift. Hence, depending on the accuracy of the solution pK_a calculations (see Experimental Procedures for a discussion of this point), E6 in the native enzyme may be partially protonated, while E10 in the K10E substitution is likely protonated. The pK_a shifts for glutamates at other positions, for example, 11 and 16 (Table 1, rows 5 and 6), are small because these residues are located at the periphery of the IBS (Figure 4A) and, hence, may experience less desolvation and electrostatic repulsion upon membrane association. In the case of the double substitution, K10E/K11E, a calculated "effective pK_a shift" (Table 1, row 2) does not have physical meaning, per se, but rather indicates how much more favorably the doubly protonated state would bind a PS membrane than the unprotonated state. In this case, we predict that the membrane association of the double substitution with both glutamates protonated is more favorable by ∼7 kcal/mol than the unprotonated form. Finally, as a control, we calculated ΔpK_a for the K54E substitution, which is located on the face of the enzyme opposite to the IBS. As expected, a negligible shift is predicted (last row, Table 1), since this residue is far from the membrane surface (i.e., on the opposite side of the enzyme that is illustrated in Figure 4A).

We performed a series of similar calculations for the hGIIA sPLA2. As depicted in Table 2, pK_a shifts of magnitudes even larger than those calculated for AppD49 are predicted for glutamates on the IBS (Figure 4B). In particular, ΔpK_a for E17 is very high both in the context of the native enzyme (4.0; Table 2, row 1) and in the context of enzymes with charge-neutralized (R7G/K10G) and charge-reversal (R7E/K10E/K16E) substitutions (3.5−4.0; Table 2, rows 2 and 3) leading to membrane-associated pK_a's of 2.2 + 4 ∼ 6.2, 4.0 + 3.5 = 7.5, and 4.0 + 4.0 = 8.0, respectively. Hence, when the positive charge on the IBS is reduced, the probability that E17 is protonated increases significantly; that is, the membrane-associated pK_a is predicted to increase from 6.2 to 7.5−8.0. Overall, the same trends observed for AppD49 sPLA2 are predicted here; ΔpK_a increases as the enzyme is moved closer to the surface of negatively charged membranes, is largest for our simulated membrane-penetrated configurations, and increases with the mole percent acidic lipid in the membrane (Figure 5). In addition, a large pK_a shift is predicted for H6 in the native enzyme (ΔpK_a = 2.3; membrane-associated pK_a = 5.4 + 2.3 = 7.7). H6 is centrally located on the IBS (Figure 4B) and is, thus, likely protonated and positively charged upon membrane association.

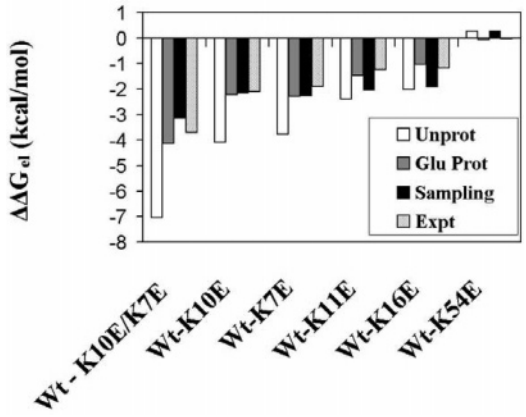

FIGURE 6: Comparison of the calculated differences in electrostatic free energies of interaction between native AppD49 sPLA2 and charge reversal-substituted forms according to various hypotheses. Experimental electrostatic free-energy differences ("Expt", light gray bars) were obtained from a previous study on anionic membranes with 0.16 M NaCl (*34*). The calculated values include scenarios in which the substituted glutamates are (1) unprotonated and in the native minimum free-energy orientation ("Unprot", white bars); (2) protonated and in the native minimum free-energy orientation ("Glu Prot", dark gray bars); and (3) unprotonated but in a minimum free-energy orientation predicted based on sampling the substituted form ("Sampling", black bars). Electrostatic free energies of interaction were calculated with a PS membrane and ionic strength of 0.1 M KCl.

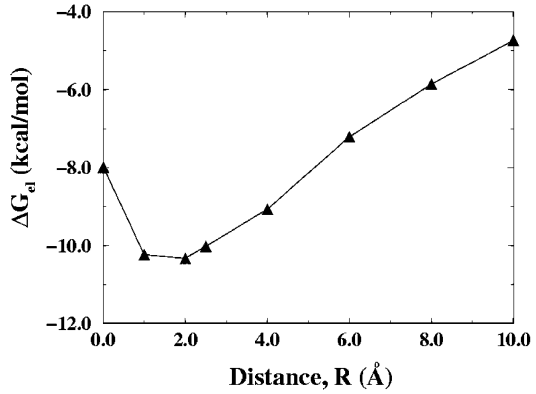

FIGURE 7: Nonspecific electrostatic contribution to the membrane association of the surface of hGIIA sPLA2 opposite the IBS. The electrostatic free energy of interaction with a PS membrane was calculated as a function of the distance between the van der Waals surfaces of the enzyme and the membrane in 0.1 M KCl.

Models for the Membrane Association of Charge-Reversal Forms of AppD49 and hGIIA sPLA2's. Combining our results on the electrostatic component of the membrane association of the native enzymes with the pK_a shift analysis of engineered glutamates, we analyzed the effect of changes in the protonation states of the glutamates on the minimum electrostatic free-energy orientations of the enzymes at the membrane surface and compared the predictions with experimental measurements. We used the FDPB method to test explicitly three possibilities: (1) glutamates on the IBS do not become protonated upon membrane association, and the minimum electrostatic free-energy orientation is the same as that previously predicted; (2) glutamates on the IBS become protonated upon membrane association, and the minimum electrostatic free-energy orientation is the same as that previously predicted; and (3) glutamate-substituted enzymes do not become protonated but assume different minimum free-energy orientations than those predicted for the native enzymes. Note, however, that, since in the experimental studies the residue-substituted enzymes are still catalytically competent, it is unlikely that their membrane-associated orientations change significantly from those of the native enzymes.

Our results are displayed in Figure 6 for AppD49 sPLA2, where $\Delta\Delta G_{el} = \Delta G_{el}$(wt) $- \Delta G_{el}$(engineered enzyme). The light gray bars represent the experimentally derived values from the study by Han et al. (*34*). The experiments were performed with 0.16 M KCl, while the calculations were performed with 0.1 M KCl. However, in all cases, relatives differences, $\Delta\Delta G_{el}$, are considered. As depicted by the white bars, which represent condition 1 in which the glutamates are not protonated and the substituted enzyme retains the same minimum free-energy orientation as the native enzyme, the calculations predict too positive or unfavorable a value for ΔG_{el}(engineered enzyme), the electrostatic free energy of the substituted enzymes; that is, likely either the enzyme changes orientation or an IBS glutamate is protonated (or a combination of both). The other two conditions, assuming either that the glutamates are protonated (dark gray bars) or that the substituted enzymes assume a slightly different orientation than the native enzymes (black bars), produce better agreement with experimental data. In particular, taking computational uncertainty into account (see Experimental Procedures), the protonation model (dark gray bars) appears to be, overall, the more adequate model. A similar extensive analysis for hGIIA sPLA2 was not performed because of a lack of experimental data due to the in vitro aggregation behavior of this enzyme (see below). However, calculations for one of the hGIIA sPLA2 substitutions, for which there is clean experimental data, also predict significantly better agreement with experimental observations when the substituted glutamate was protonated (data not shown). The electrostatic free-energy results discussed above, in addition to the pK_a shift analysis, support our hypothesis that specific residues in close proximity to the membrane surface upon association may change their protonation states. Alternatively, our calculations are consistent with a model in which the glutamates are not protonated but assume new minimum free-energy orientations (Figure 6, black bars).

In some cases, better agreement with experimental data may be achieved if both scenarios (protonation and re-sampling) are taken into account. For example, as seen in Figure 6, the protonation model produces much better agreement with experimental data than the sampling model for K16E. However, E16 is still in very close proximity to the membrane surface for the re-sampled orientation, and may, thus, become protonated. Assuming E16 becomes protonated after sampling in this engineered enzyme significantly improves agreement with experimental data: $\Delta\Delta G_{el}$ (Expt) $= -1.2$ kcal/mol and $\Delta\Delta G_{el}$ (Sampling) $= -1.9$ kcal/mol; however, $\Delta\Delta G_{el}$ (Sampling then Glu Prot) $= -1.2$ kcal/mol. This suggests that protonation and reorientation may work in concert to produce the final membrane-associated state.

Mechanistic Model for the Formation of Supramolecular Aggregates Involving Human Group IIA sPLA2 and Anionic Membranes. Experimental studies based on continuous wave and time domain electron paramagnetic resonance (EPR) spectroscopy and light scattering (*56*) show that the hGIIA

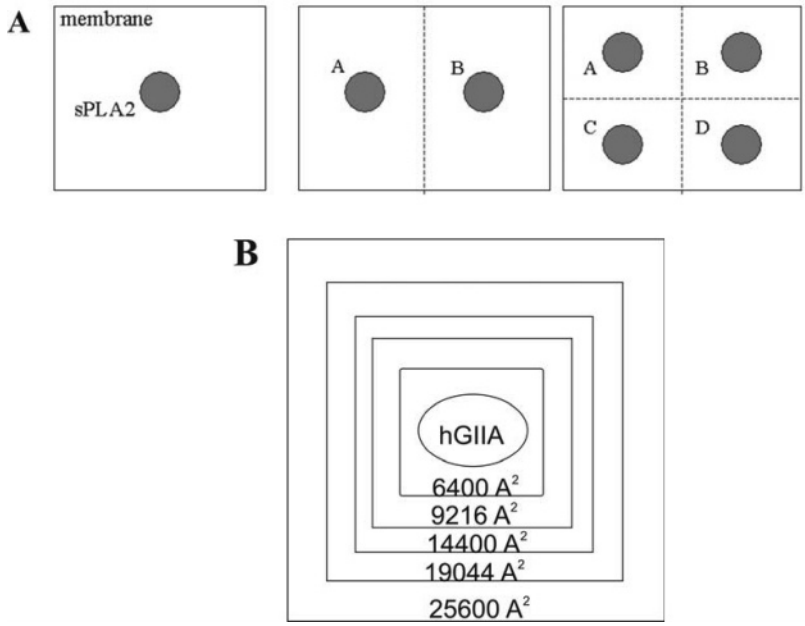

FIGURE 8: Schematic representations of the configurations used for the calculation of the electrostatic component of the membrane aggregation induced by hGIIA sPLA2. (A) First scenario: the first membrane surface is represented as a rectangle to which hGIIA sPLA2's (represented as spheres A, B, C, and D) are pre-bound in their minimum free-energy orientations. The second membrane, which is brought near this complex and binds the upper surfaces of the enzymes, is not shown for clarity. (B) Second scenario: the change in membrane surface area per sPLA2 is represented as rectangles of decreasing areas, and hGIIA sPLA2 is represented as an ellipse.

sPLA2 forms supramolecular complexes with anionic phospholipids vesicles. Because the phenomenon was not observed for sPLA2's with a significantly less basic character (e.g., bvPLA2 has a pI ∼ 5.8 versus hGIIA sPLA2 which has a pI ∼ 9.5) and because anionic phospholipids are required, it was suggested that electrostatic interactions are involved in this process. As indicated by the electrostatic potential calculations in Figure 1B and described above, hGIIA sPLA2 has a surface, located on the opposite side of the enzyme from the IBS, which is expected to interact strongly with PS membranes. But unlike the IBS, this surface lacks hydrophobic residues, and hence, its interaction with membranes is likely driven solely by electrostatic interactions. We calculated the electrostatic free energy of interaction with a PS membrane (in 0.1 M KCl) for the enzyme in an orientation that is rotated 180° about an axis perpendicular to the plane of the page with respect to the orientation depicted in Figure 1B. The calculated electrostatic free energy curve (Figure 7) has a minimum ΔG_{el} similar to that depicted by the curve in Figure 2 (triangles) for the IBS. The ability of this enzyme to interact strongly with anionic membranes through more than one surface has been suggested as a possible mechanism for the observed aggregation (*29*, *56*). Here, we propose a minimal model for enzyme-induced aggregation and examine quantitatively whether favorable electrostatic interactions between membranes and both surfaces of hGIIA sPLA2 are indeed sufficient to overcome the large electrostatic repulsions experienced between two "undressed", that is, enzyme-free, negatively charged membrane surfaces.

We considered the electrostatic free energy of a protein−membrane "aggregate complex", such as that shown in Figure 10, consisting of the two opposite surfaces of hGIIA sPLA2 (Figures 1, 2, and 7) adsorbed to two apposing PS (or 2:1 PC/PS) membranes. The electrostatic free energy of aggregation (ΔG_{el}(aggregation); eq 3) is calculated for the

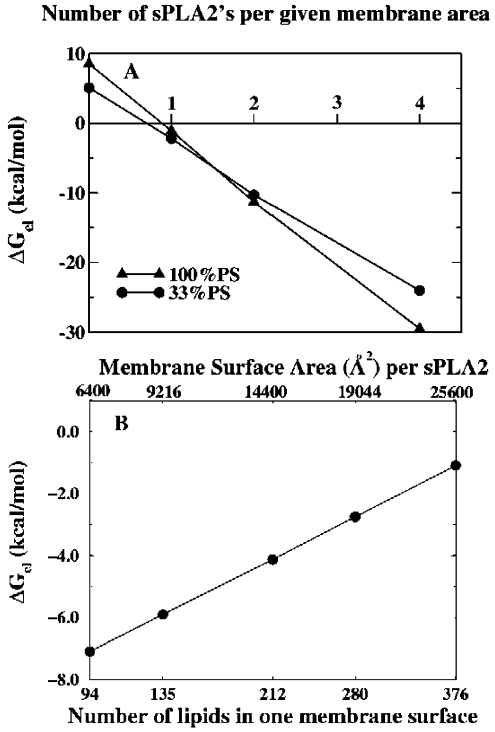

FIGURE 9: The electrostatic free energy of hGIIA sPLA2-induced membrane aggregation, ΔG_{el}(aggregation). (A) ΔG_{el}(aggregation) as a function of the number of enzymes per constant membrane surface area; the calculations are based on the scheme outlined in Figure 8A. (B) ΔG_{el}(aggregation) as a function of the membrane surface area for a single enzyme; the calculations are based on the scheme outlined in Figure 8B. The FDPB calculations were performed with either PS or 2:1 PC/PS membranes with 0.1 M KCl.

two scenarios depicted schematically in Figures 8. In all cases, the envelopes of the apposed membrane surfaces are ∼40 Å apart; this distance accommodates the height of the enzyme plus ∼2 Å on either side between the van der Waals

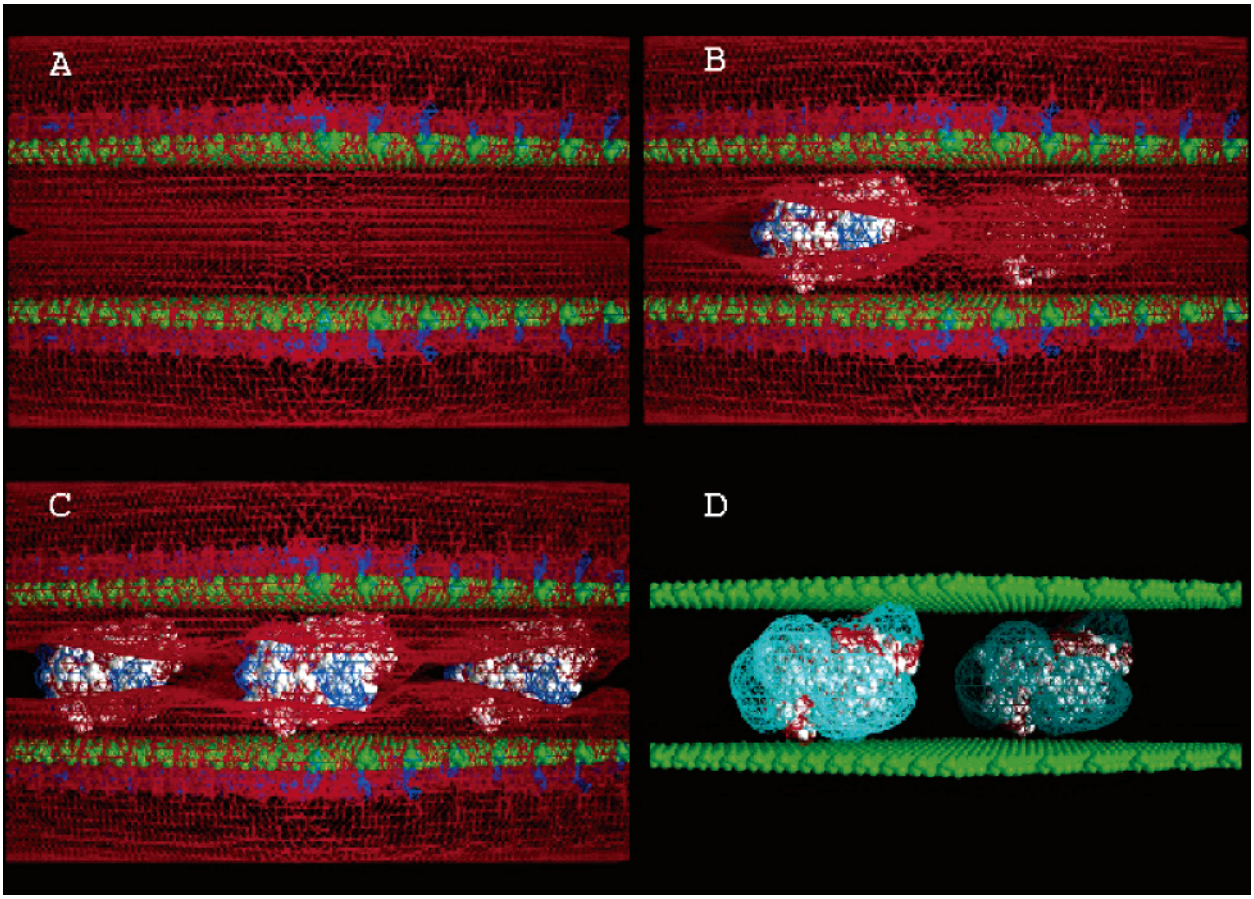

FIGURE 10: Qualitative illustration of the electrostatic forces involved in hGIIA sPLA2-induced membrane aggregation. Blue (red) meshes represent the +1 kT/e (−1 kT/e) equipotential contours as calculated by the FDPB method for 0.1 M KCl and visualized in GRASP (*51*). The calculations were preformed with PS membranes and 0.1 M KCl. (A) Two opposed PS membranes experience a large electrostatic repulsion in the absence of enzyme. Two (B) or four (C) hGIIA enzymes, represented by their molecular surfaces (white), are sandwiched between the membranes, as described in the text. In the presence of enzyme, the electrostatic repulsion between the two membranes is reduced, and the membrane/protein/membrane system is stabilized by favorable protein/membrane interactions. (D) Difference map obtained by subtracting the electrostatic potentials in panel B from those in panel A (cyan represents the +0.5 kT/e equipotential contour). Because of discreteness of charge effects, the enzymes do not merely neutralize the membrane surfaces but contribute additional favorable electrostatic interactions.

surfaces of the enzyme and membranes. The values for ΔG_{el}-(aggregation) denote the change in electrostatic free energy upon bringing the second membrane to its final position, either in the absence ($N = 0$) or presence ($N > 0$) of enzyme-(s).

In each scenario depicted in Figure 8A, the lateral membrane surface area is invariant, and ΔG_{el}(aggregation) was calculated as a function of the number of enzymes adsorbed to the membrane surfaces (Figure 9A). In the absence of enzyme, the repulsion, even at an intermembrane separation of 4 D lengths, is quite large, ranging between ∼+5 to +10 kcal/mol for 2:1 PC/PS and PS membranes, respectively. The introduction of a single enzyme dramatically reduces this repulsion. Additional enzymes were included so that the protein/protein interaction free energies, both in the absence and presence of membrane, are negligible (calculations not shown).This ensures that protein/protein repulsion does not counterbalance the favorable protein/membrane interaction calculated by eq 3. As the number of enzymes increases, the electrostatic free energy of aggregation becomes dramatically more favorable. These results indicate that (1) electrostatic interactions alone can drive aggregation and (2) the surface density of enzyme required for aggregation can be relatively low, that is, [P] < [L]. This is illustrated more quantitatively in Figure 9B, which is based on the calculations depicted schematically in Figure 8B; one enzyme per 280, 212, or 135 lipids (per one leaflet) significantly reduces the electrostatic repulsion between undressed PS membranes and results in calculated electrostatic free energies of aggregation of −3, −4, or −6 kcal/mol, respectively (Figure 9B). Our predicted required minimum surface density (∼ one protein per 20 000 Å^2) is in good agreement with estimates based on experimental studies (*56*).

Figure 10 illustrates qualitatively the aggregating effect of hGIIA sPLA2 on two apposed PS membranes. Figure 10A shows the equipotential potential profiles in the absence of enzyme, and Figure 10B depicts the corresponding potential profiles in the presence of enzymes oriented so that their two membrane binding surfaces are simultaneously adsorbed to both membranes. In Figure 10A, the −1 kT/e (−25 mV) negative potential contours from each membrane (red meshes) overlap each other and produce the strong repulsion calculated in Figure 9A ($N = 0$). In Figure 10B,C, the strong, localized positive potential associated with each enzyme (blue meshes, +1 kT/e, +25 mV) creates an electrostatically favorable condition; this is illustrated by the potential difference map of Figure 10D (cyan mesh, +0.5 kT/e, +12.5

mV), which shows that the system in panel B has a more positive character than that of panel A. Thus, due to the "discreteness of charge effect" seen in many other systems, the enzymes in panels B and C do not merely neutralize the membrane/membrane electrostatic repulsion, but also produce favorable protein/membrane interactions.

Our model predicts that enzymes will be recruited to regions of membrane/membrane contact until the enzyme/enzyme repulsion out-competes the favorable enzyme/membrane attraction. This supports the hypothesis that the enzymes in the observed aggregates are in "close proximity" (*56*). Our results clearly illustrate the central role of nonspecific electrostatics and provide a quantitative model for the formation of hGIIA sPLA2/membrane supramolecular complexes. The overall dramatic basic character of hGIIA sPLA2 facilitates the enzyme-induced membrane aggregation.

DISCUSSION

As a family, secreted phospholipases A2 (sPLA2's) exhibit a rich diversity in membrane binding behavior despite high sequence and structure similarity (*12*, *14*, *28*). The residue character of the interfacial binding surface (IBS) of these enzymes appears to define the unique admixture of electrostatic and hydrophobic properties responsible for nonspecific membrane selectivity. Because of the complex, and often subtle, interplay between these simple physical interactions, especially upon alterations in the physical characteristics of the system, for example, residue substitutions on the IBS, membrane composition, and ionic strength, it has been difficult to tease out the contribution of each of the individual components experimentally. Our computational approach to this problem, which is based on well-defined physical principles, and the comparison of our predictions with experimental observations have helped elucidate the quantitative mechanistic role of electrostatics in the membrane association of Group II sPLA2's.

Specifically, we examined the experimentally and structurally well-characterized enzymes AppD49 and hGIIA sPLA2's. Both have a significant number of basic residues on the IBS, which interact strongly with membrane surfaces that are negatively charged through favorable electrostatic interactions (*31*, *34*). Our calculations show that even under conditions of high desolvation, when the IBS is in close apposition to the membrane interface, that is, the conditions expected during lipid catalysis, there is still a significantly favorable electrostatic component that may act cooperatively with the interfacial penetration of hydrophobic residues on the IBS (see Figure 2, $R = 0$ Å). It is interesting to compare this result with our recent analysis of the Group III bee venom sPLA2 (bvPLA2) (*39*). In this case, electrostatics was correctly predicted to play a relatively minor role in terms of its contribution to the free energy of binding and was attributed to the presence of two basic residues located close to the membrane surface, as inferred from EPR studies (*62*), while other basic residues, which are located further from the catalytic cleft, were predicted not to contribute significantly. bvPLA2 has a net charge of +4, while AppD49 and hGIIA sPLA2's have net charges of +8 and +17, respectively. Each of these three enzymes shows a marked preference for anionic membranes, albeit at different degrees. When the surface characteristics of these enzymes is compared with sPLA2's that have high affinity for neutral vesicles, such as human Group X (*63*) and cobra venom (*Naja naja naja*) (*64*) sPLA2's, which are overall acidic, we find that the IBS of each enzyme contains a similar number of hydrophobic residues, but the electrostatic potential profiles of the IBS regions are dramatically different. The magnitude of the potential profiles of the IBS regions of human Group X and cobra venom sPLA2's is similar to that of bvPLA2 but is significantly diminished with respect to the magnitude of the profiles surrounding the IBS of AppD49 and hGIIA sPLA2's. However, the profiles of the former are negative, while those of the latter three enzymes are positive. In addition, the positive profile on the IBS of AppD49 sPLA2 is weaker than that of hGIIA sPLA2 (Figure 1). These observations have a number of implications: (1) Those enzymes with the diminished profiles, negative or positive, that is, human Group X and both cobra and bee venom sPLA2's, will have a relatively enhanced ability to associate with electrically neutral membranes in a catalytically competent mode because the nonpolar interactions due to the insertion of their IBS hydrophobic residues into the membrane interface are sufficient to overcome the relatively minor electrostatic desolvation. (2) Those enzymes with diffuse negative potentials on their IBS, that is, Group X and cobra venom sPLA2's, will select against anionic membranes due to charge−charge repulsions with acidic phospholipids. (3) Those enzymes with any amount of positive potential surrounding the IBS, that is, human Group IIA, AppD49, and bee venom sPLA2's, will exhibit selectivity for anionic membranes due to charge−charge attractions. Thus, for example, bvPLA2, which has a diminished positive potential surrounding its IBS, exhibits the ability to bind to both neutral and anionic membranes because of the unique basic/hydrophobic character of its IBS. At least in the case of AppD49 sPLA2, it has been shown that the binding mode is affected according to the anionic property of the membrane (*30*). The computational analysis stresses the importance of the location of the membrane-interacting residues and the physical character of the IBS that gives each enzyme its unique binding behavior. The composition of the membrane and the ionic strength are also important determinants of membrane binding ability.

Generally, charge reversal substitutions, specifically changing basic residues to glutamates, have been used in the analysis of the membrane association of sPLA2's to elucidate the contribution of particular basic residues to the membrane association of the native enzyme (*31*, *34*, *65*). Our computational analysis suggests that charge reversal substitutions can affect membrane association in ways which may complicate the interpretation of such contributions. Figure 5 indicates that native glutamates (E6 in AppD49 sPLA2 and E17 in hGIIA sPLA2) may become protonated upon membrane association and that the pK_a shifts required for protonation may be sufficient when the membrane contains only 33 mol % acidic lipid, a composition that has been used in the experimental analysis of these enzymes. Our calculations further indicate that similar considerations may hold for charge reversal substitutions (Tables 1 and 2). Indeed, the protonation of glutamates has been observed in other systems as well: (1) In the case of Saposin C, a small glycoprotein, neutralization of glutamates on its membrane

binding surface is essential for its fusogenic function (*61*). (2) Glutamates on an amphipathic α-helix of Cytidylyltransferase regulate membrane association by becoming protonated and inducing membrane association only in the presence of acidic lipids (*66*). (3) Our previous analysis of glutamate-substituted forms of bvPLA2 (*39*) illustrated pH-dependent differences in membrane binding affinity; this was attributed to the pH-dependent protonation of only one or two out of five glutamates on the IBS of a glutamate-engineered form of the enzyme. Hence, it is clear that it is necessary to consider changes in the ionic states of residues located on the membrane binding surfaces of peripheral proteins upon membrane adsorption.

Our calculations also provide alternative models for how the charge substitution forms of sPLA2's may associate with anionic membranes. As illustrated in Figure 6 for AppD49 sPLA2, the calculated change in electrostatic free energies of membrane interaction for charge reversal substitutions in which the substituted glutamates are protonated (dark gray bars) or whose orientations are in their respective minimum electrostatic free-energy orientations (black bars) correlates better with experimental observations (light gray bars) than with the assumption that the engineered enzymes adopt the same membrane-associated orientations as the native enzymes (white bars) (*31*, *34*). Hence, our calculations are consistent either with the enzymes adopting orientations that differ slightly from the native orientations (Figure 6, black bars) or with an engineered glutamate becoming protonated (dark gray bars), thus, relieving the charge−charge repulsion set up upon membrane association. Depending on the electrostatic characteristics of the IBS and the membrane interface, nonpolar interactions (mediated by hydrophobic residues on the IBS) exert an influence in contributing to the final membrane-associated orientation. The overall agreement of our predicted membrane-associated models, based on the consideration of electrostatic interactions alone, with indirect experimental observations of the docking of these enzymes to membrane interfaces (*56*, *62*), indicates that for hGIIA sPLA2 electrostatic interactions are a main driving force or that the membrane binding characteristics of the electrostatic aspects of the IBS are consistent with the hydrophobic aspects. For the determination of the catalytically competent membrane-associated orientation of AppD49 sPLA2, electrostatic interactions appear to play a more important role when the membrane contains greater than 20 mol % acidic lipid, whereas hydrophobic contributions likely dominate at lower anionic lipid concentrations.

Last, our calculations provide a quantitative model for how electrostatic interactions can induce the experimentally observed aggregation of hGIIA sPLA2's in the presence of anionic vesicles. Two electrostatically equivalent orientations for the hGIIA enzyme (Figures 1B, 2, and 7) are predicted: (1) an interaction with the membrane surface through the IBS and (2) an interaction through the surface opposite the IBS. Thus, membrane-associated hGIIA sPLA2 might exist in a dynamic equilibrium between these two orientations. Since only the IBS has a significant proportion of interfacially associating hydrophobic residues, it is likely the preferred membrane binding surface as observed in EPR studies (*56*). Generally, the opposite face of the enzyme is free to interact with a second membrane, and this would be facilitated if the lipid concentration is sufficiently high. Our results predict an approximate surface density of sPLA2's required to aggregate two PS membranes; one hGIIA sPLA2 per 144 nm^2 or 212 lipids (per each vesicle surface) produces an electrostatic free energy of aggregation of −4 kcal/mol (Figure 9B). Higher surface densities produce more favorable free energies of aggregation (Figure 9). The EPR data (*56*) predicts patches of enzymes that are sandwiched between vesicles, similar to the complexes depicted in Figure 10. However, the physiological significance of electrostatic-induced aggregation is not clear. One role may be related to the activity of hGIIA sPLA2 against bacteria which have a highly negatively charged surface layer (*56*). Another may be related to atherosclerosis. Intriguingly, hydrolysis of low-density lipoproteins by hGIIA sPLA2, and more recently Group V sPLA2, has been implicated in particle aggregation (*71*, *72*). Such particle fusion is thought to promote atherosclerosis (*71*). For hGIIA sPLA2, particle aggregation may be mediated by the mechanism outlined here. However, there is no structure available for a Group V sPLA2. We built a comparative model for rat Group V sPLA2 (SwissProt accession number P51433; see Figure S2 in Supporting Information). The magnitude of the electrostatic potential of the IBS on the Group V model is predicted to be smaller and overall less positive than the hGIIA sPLA2, but the model predicts that there is a similar, large lobe of positive potential on the "backside" of the enzyme as shown in Figure 1B. This is a characteristic that the Group V enzyme may share in common with hGIIA sPLA2, and hence, the Group V enzyme may similarly induce anionic vesicle aggregation (Figure 10). Our model, although simplistic, suggests that electrostatics may play a role in LDL particle aggregation (*71*).

Molecular dynamics (MD) simulations have been used previously to study the membrane association behavior of hGIIA sPLA2 (*69*) and the effect of hydrolysis products on the integrity and electrostatic properties of membranes (*70*). With simulations, Zhou and Schulten (*69*) found that (1) the conformation of hGIIA sPLA2 did not change appreciably at the membrane surface over the course of the simulation period (120 ps) and (2) significant desolvation occurred only for hydrophobic residues on the IBS. The former result supports our use of a static model for the enzyme, although the simulations were relatively short, and the latter result supports our model for calculating pK_a shifts of glutamate-substituted enzymes, that is, that the enzyme is surface-adsorbed. Hyvonen et al. (*70*) used 1-ns simulations to predict that membranes consisting of sPLA2-hydrolyzed lipid products have a "loosened structure" with respect to unhydrolyzed membranes, which suggests a model for the experimentally observed hydrolysis product-induced activation of sPLA2's. However, these studies also showed that the surface potential of membranes composed of negatively charged hydrolysis products is over-attenuated by counterions and the strongly enhanced ordering of water molecules, which is due to effects related to truncation of electrostatic forces in the simulations. While our calculations do not account for lipid motions, they accurately represent electrostatic interactions. A further advantage of our approach is the ability to examine, with currently available computational resources, a comprehensive range of conditions, that is, different membrane compositions, ionic strengths, residue substitutions, and relative orientations of the enzyme with respect to the membrane. In future work,

time frames from MD simulations of sPLA2/membrane systems will be examined with the continuum methods described in this study to more accurately account for lipid-mediated effects. Preliminary work with model systems is currently under way.

Overall, we hypothesize models for the membrane binding behaviors of these two enzymes. AppD49 sPLA2 has a nearly dipolar potential profile with positive potential concentrated about the IBS (Figure 1A). This enzyme is recruited to negatively charged membranes through nonspecific electrostatic interactions. Electrostatic forces orient the enzyme at the membrane surface, which facilitates the penetration of hydrophobic residues on the IBS. Very likely, the native E6 is protonated upon interfacial binding, further increasing membrane association through the decrease in both charge−charge repulsion with acidic lipids and desolvation repulsion of the charged residue now protonated. In contrast, the potential profile of hGIIA sPLA2 is almost completely basic (Figure 1B), giving rise to the vesicle aggregation behavior discussed above. For hGIIA sPLA2, two residues on the native IBS are likely protonated: (1) E17, for which similar considerations apply as discussed above in regard to E6 of AppD49 sPLA2, and (2) H6, which likely becomes positively charged and, thus, contributes to the electrostatic binding through attraction to acidic lipids. In the case of glutamate-engineered forms of both sPLA2's, we predict that the enzymes experience a slight change in orientation at the membrane surface, relative to the native enzymes, as well as protonation of the engineered glutamates once the enzymes assume a catalytically competent orientation, which is closer to the minimum free-energy orientation of the native enzyme and would, thus, bring these residues closer to the membrane interface. We note that, for both enzymes, protonation, which is dependent on the acidic lipid concentration of the membrane, may be an important factor in orienting the enzymes optimally for catalysis. Under physiological conditions, the change in acidic lipid content will be contributed by the accumulation of fatty acids as a result of lipid hydrolysis. The enzyme, thus, probably exhibits multiple dynamic binding states that are dictated by the biophysical nature of both the protein and the membrane surface.

SUPPORTING INFORMATION AVAILABLE

Work referred to in the text regarding the calculation of intrinsic pK_a's of titratable amino acids in sPLA2's and the construction of the comparative model for the rat Group V sPLA2. This material is available free of charge via the Internet at http://pubs.acs.org.

REFERENCES

1. Cho, W., and Stahelin, R. V. (2005) Membrane-protein interactions in cell signaling and membrane trafficking, *Annu. Rev. Biophys. Biomol. Struct. 34*, 119−151.
2. DiNitto, J. P., Cronin, T. C., and Lambright, D. G. (2003) Membrane recognition and targeting by lipid-binding domains, *Sci STKE, 2003*(213), re 16.
3. Murray, D., Arbouzova, A., Honig, B., and McLaughlin, S. (2002) The role of electrostatic and nonpolar interactions in the association of peripheral proteins with membranes, in *Current Topics in Membranes: Peptide−Lipid Interactions* (Simon, S., and McIntosh, T., Eds.) pp 278−309, Academic Press, San Diego, CA.
4. Arbuzova, A., Murray, D., and McLaughlin, S. (1998) MARCKS, membranes and calmodulin: kinetics of interaction, *Biochim. Biophys. Acta 1376*, 369−379.
5. Buser, C. A., Sigal, C. T., Resh, M. D., and McLaughlin, S. (1994) Membrane binding of myristylated peptides corresponding to the NH_2-terminus of Src, *Biochemistry 33*, 13093−13101.
6. Ghomashchi, F., Zhang, X., Liu, L., and Gelb, M. H. (1995) Binding of prenylated and polybasic peptides to membranes: affinities and intervesicle exchange, *Biochemistry 34*, 11910−11918.
7. Hancock, J. F., Paterson, H., and Marshall, C. J. (1990) A polybasic domain or palmitoylation is required in addition to the CAAX motif to localize p21ras to the plasma membrane, *Cell 63*, 133−139.
8. Zhou, W., Parent, L. J., Wills, J. W., and Resh, M. D. (1994) Identification of a membrane-binding domain within the amino-terminal region of human immunodeficiency virus type 1 Gag protein which interacts with acidic phospholipids, *J. Virol. 68*, 2556−2569.
9. McLaughlin, S., and Aderem, A. (1995) The myristoyl-electrostatic switch: a modulator of reversible protein−membrane interactions, *Trends Biochem. Sci. 20*, 272−276.
10. Hurley, J. H., and Meyer, T. (2001) Subcellular targeting by membrane lipids, *Curr. Opin. Cell Biol. 13*, 146−152.
11. McDermott, M., Wakelam, M. J., and Morris, A. J. (2004) Phospholipase D, *Biochem. Cell Biol. 80*, 225−253.
12. Gelb, M. H., Cho, W., and Wilton, D. C. (1999) Interfacial binding of secreted phospholipases A(2): more than electrostatics and a major role for tryptophan, *Curr. Opin. Struct. Biol. 9*, 428−432.
13. McLaughlin, S., and Murray, D. (2005) Plasma membrane phosphoinositide organization by protein electrostatics, *Nature 438*, 605−611.
14. Six, D. A., and Dennis, E. A. (2000) The expanding superfamily of phospholipase A2 enzymes: classification and characterization, *Biochim. Biophys. Acta 1488*, 1−19.
15. Berg, O. G., Gelb, M. H., Tsai, M. D., and Jain, M. K. (2001) Interfacial enzymology: the secreted phospholipase A(2)-paradigm, *Chem. Rev. 101*, 2613−2654.
16. Ramirez, F., and Jain, M. K. (1991) Phospholipase A2 at the bilayer interface, *Proteins 9*, 229−239.
17. Murakami, M., and Kudo, I. (2002) Phospholipase A2, *J. Biochem. (Tokyo) 131*, 285−292.
18. Yedgar, S., Lichtenberg, D., and Schnitzer, E. (2000) Inhibition of phospholipase A(2) as a therapeutic target, *Biochim. Biophys. Acta 1488*, 182−187.
19. Chakraborti, S. (2003) Phospholipase A(2) isoforms: a perspective, *Cell. Signalling 15*, 637−665.
20. Ward, R. J., de, A. W., Jr., and Arni, R. K. (1998) At the interface: crystal structures of phospholipases A2, *Toxicon 36*, 1623−1633.
21. Arni, R. K., and Ward, R. J. (1996) Phospholipase A2−a structural review, *Toxicon 34*, 827−841.
22. Biltonen, R. L., Heimburg, T. R., Lathrop, B. K., and Bell, J. D. (1990) Molecular aspects of phospholipase A2 activation, *Adv. Exp. Med. Biol. 279*, 85−103.
23. Honger, T., Jorgensen, K., Stokes, D., Biltonen, R. L., and Mouritsen, O. G. (1997) Phospholipase A2 activity and physical properties of lipid-bilayer substrates, *Methods Enzymol. 286*, 168−190.
24. Scott, D. L., White, S. P., Otwinowski, Z., Yuan, W., Gelb, M. H., and Sigler, P. B. (1990) Interfacial catalysis: the mechanism of phospholipase A2, *Science 250*, 1541−1546.
25. Canaan, S., Zadori, Z., Ghomashchi, F., Bollinger, J., Sadilek, M., Moreau, M. E., Tijssen, P., and Gelb, M. H. (2004) Interfacial enzymology of parvovirus phospholipases A2, *J. Biol. Chem. 279*, 14502−14508.
26. Kinkaid, A. R., and Wilton, D. C. (1994) Comparison of the properties of human group II phospholipase A2 with other secretory phospholipases, *Biochem. Soc. Trans. 22*, 315S.
27. Koduri, R. S., Gronroos, J. O., Laine, V. J., Le Calvez, C., Lambeau, G., Nevalainen, T. J., and Gelb, M. H. (2002) Bactericidal properties of human and murine groups I, II, V, X, and XII secreted phospholipases A(2), *J. Biol. Chem. 277*, 5849−5857.
28. Scott, D. L., Mandel, A. M., Sigler, P. B., and Honig, B. (1994) The electrostatic basis for the interfacial binding of secretory phospholipases A2, *Biophys. J. 67*, 493−504.
29. Bezzine, S., Bollinger, J. G., Singer, A. G., Veatch, S. L., Keller, S. L., and Gelb, M. H. (2002) On the binding preference of human groups IIA and X phospholipases A2 for membranes with anionic phospholipids, *J. Biol. Chem. 277*, 48523−48534.

30. Gadd, M. E., and Biltonen, R. L. (2000) Characterization of the interaction of phospholipase A(2) with phosphatidylcholine-phosphatidylglycerol mixed lipids, *Biochemistry 39*, 9623−9631.
31. Snitko, Y., Han, S. K., Lee, B. I., and Cho, W. (1999) Differential interfacial and substrate binding modes of mammalian pancreatic phospholipases A2: a comparison among human, bovine, and porcine enzymes, *Biochemistry 38*, 7803−7810.
32. Maraganore, J. M., and Heinrikson, R. L. (1993) The lysine-49 phospholipase A2 from the venom of *Agkistrodon piscivorus piscivorus*. Relation of structure and function to other phospholipases A2, *J. Biol. Chem. 268*, 6064.
33. Snitko, Y., Koduri, R. S., Han, S. K., Othman, R., Baker, S. F., Molini, B. J., Wilton, D. C., Gelb, M. H., and Cho, W. (1997) Mapping the interfacial binding surface of human secretory group IIa phospholipase A2, *Biochemistry 36*, 14325−14333.
34. Han, S. K., Yoon, E. T., Scott, D. L., Sigler, P. B., and Cho, W. (1997) Structural aspects of interfacial adsorption. A crystallographic and site-directed mutagenesis study of the phospholipase A2 from the venom of *Agkistrodon piscivorus piscivorus*, *J. Biol. Chem. 272*, 3573−3582.
35. Gallagher, K., and Sharp, K. A. (1998) Electrostatic contributions to heat capacity changes of DNA-ligand binding, *Biophys. J. 75*, 769−776.
36. Honig, B., and Nicholls, A. (1995) Classical electrostatics in biology and chemistry, *Science 268*, 1144−1149.
37. Ben Tal, N., Honig, B., Peitzsch, R. M., Denisov, G., and McLaughlin, S. (1996) Binding of small basic peptides to membranes containing acidic lipids: theoretical models and experimental results, *Biophys. J. 71*, 561−575.
38. Murray, D., Hermida-Matsumoto, L., Buser, C. A., Tsang, J., Sigal, C., Ben Tal, N., Honig, B., Resh, M. D., and McLaughlin, S. (1998) Electrostatics and the membrane association of Src: theory and experiment, *Biochemistry 37*, 2145−2159.
39. Bollinger, J. G., Diraviyam, K., Ghomashchi, F., Murray, D., and Gelb, M. H. (2004) Interfacial binding of bee venom secreted phospholipase A2 to membranes occurs predominantly by a nonelectrostatic mechanism, *Biochemistry 43*, 13293−13304.
40. Murray, D., and Honig, B. (2002) Electrostatic control of the membrane targeting of C2 domains, *Mol. Cell 9*, 145−154.
41. Sharp, K. A., and Honig, B. H. (1990) Calculating total electrostatic energies with the nonlinear Poisson−Boltzmann equation, *J. Phys. Chem. 94*, 7684−7692.
42. Scott, D. L., White, S. P., Browning, J. L., Rosa, J. J., Gelb, M. H., and Sigler, P. B. (1991) Structures of free and inhibited human secretory phospholipase A2 from inflammatory exudate, *Science 254*, 1007−1010.
43. Shindyalov, I. N., and Bourne, P. E. (1998) Protein structure alignment by incremental combinatorial extension (CE) of the optimal path, *Protein Eng. 11*, 739−747.
44. Brooks, B. R., Bruccoleri, R. E., Olafson, B. D., States, D. J., Swaminathan, S., and Karplus, M. (1983) CHARMM: a program for macromolecular energy, minimization, and dynamics calculations, *J. Comput. Chem. 4*, 187−217.
45. Peitzsch, R. M., Eisenberg, M., Sharp, K. A., and McLaughlin, S. (1995) Calculations of the electrostatic potential adjacent to model phospholipid bilayers, *Biophys. J. 68*, 729−738.
46. Sharp, K. A., and Honig, B. H. (1990) Electrostatic interactions in macromolecules: theory and applications, *Annu. Rev. Biophys. Biophys. Chem. 19*, 301−332.
47. Misra, V., and Honig, B. (1995) On the magnitude of the electrostatic contribution to ligand-DNA interactions, *Proc. Natl. Acad. Sci. U.S.A. 92*, 4691−4695.
48. Misra, V. K., Hecht, J. L., Yang, A. S., and Honig, B. (1998) Electrostatic contributions to the binding free energy of lambdacI repressor to DNA, *Biophys. J. 75*, 2262−2273.
49. Gilson, M. K., Sharp, K. A., and Honig, B. H. (1987) Calculating the electrostatic potential of molecules in solution: method and error assessment, *J. Comput. Chem. 9*, 327−335.
50. Alexov, E. G., and Gunner, M. R. (1997) Incorporating protein conformational flexibility into the calculations of pH-dependent protein properties, *Biophys. J. 2*, 2075−2093.
51. Nicholls, A., Sharp, K. A., and Honig, B. (1991) Protein folding and association: insights from the interfacial and thermodynamic proterties of hydrocarbon, *Proteins 11*, 281−296.
52. Ben Tal, N., Honig, B., Miller, C., and McLaughlin, S. (1997) Electrostatic binding of proteins to membranes: theoretical prediction and experimental results with charybdotoxin and phospholipid vesicles, *Biophys. J. 73*, 1717−1727.
53. Diraviyam, K., Stahelin, R. V., Cho, W., and Murray, D. (2003) Computer modeling of the membrane interaction of FYVE domains, *J. Mol. Biol. 328*, 721−736.
54. Singh, S. M., and Murray, D. (2003) Molecular modeling of the membrane targeting of phospholipase C pleckstrin homology domains, *Protein Sci. 12*, 1934−1953.
55. Lathrop, B., Gadd, M., Biltonen, R. L., and Rule, G. S. (2001) Changes in Ca^{2+} affinity upon activation of *Agkistrodon piscivorus piscivorus* phospholipase A2, *Biochemistry 40*, 3264−3272.
56. Canaan, S., Nielsen, R., Ghomashchi, F., Robinson, B. H., and Gelb, M. H. (2002) Unusual mode of binding of human group IIA secreted phospholipase A2 to anionic interfaces as studied by continuous wave and time domain electron paramagnetic resonance spectroscopy, *J. Biol. Chem. 277*, 30984−30990.
57. Beers, S. A., Buckland, A. G., Giles, N., Gelb, M. H., and Wilton, D. C. (2003) Effect of tryptophan insertions on the properties of the human group IIA phospholipase A2: mutagenesis produces an enzyme with characteristics similar to those of the human group V phospholipase A2, *Biochemistry 42*, 7326−7338.
58. Tatulian, S. A. (2001) Toward understanding interfacial activation of secretory phospholipase A2 (PLA2): membrane surface properties and membrane-induced structural changes in the enzyme contribute synergistically to PLA2 activation, *Biophys. J. 80*, 789−800.
59. Tatulian, S. A. (2003) Structural effects of covalent inhibition of phospholipase A2 suggest allosteric coupling between membrane binding and catalytic sites, *Biophys. J. 84*, 1773−1783.
60. Cornell, R. B., and Northwood, I. C. (2000) Regulation of CTP: phosphocholine cytidylyltransferase by amphitropism and relocalization, *Trends Biochem. Sci. 25*, 441−447.
61. de Alba, E., Weiler, S., and Tjandra, N. (2003) Solution structure of human saposin C: pH-dependent interaction with phospholipid vesicles, *Biochemistry 42*, 14729−14740.
62. Lin, Y., Nielsen, R., Murray, D., Hubbell, W. L., Mailer, C., Robinson, B. H., and Gelb, M. H. (1998) Docking phospholipase A2 on membranes using electrostatic potential-modulated spin relaxation magnetic resonance, *Science 279*, 1925−1929.
63. Pan, Y. H., Yu, B. Z., Singer, A. G., Ghomashchi, F., Lambeau, G., Gelb, M. H., Jain, M. K., and Bahnson, B. J. (2002) Crystal structure of human group X secreted phospholipase A2. Electrostatically neutral interfacial surface targets zwitterionic membranes, *J. Biol. Chem. 277*, 29086−29093.
64. Sumandea, M., Das, S., Sumandea, C., and Cho, W. (2000) Roles of aromatic residues in high interfacial activity of *Naja naja atra* phospholipase A(2), *Biochemistry 39*, 4206.
65. Lin, Y., Ghomashchi, F., Nielsen, R., Snitko, Y., Yu, B. Z., Han, S. K., Cho, W., Wilton, D. C., Jain, M. K., Robinson, B. H., and Gelb, M. H. (1998) Binding of bee venom and human group IIa phospholipases A2 to membranes: a minor role for electrostatics, *Biochem. Soc. Trans. 26*, 341−345.
66. Johnson, J. E., Xie, M., Singh, L., Edge, R., and Cornell, R. B. (2003) Both acidic and basic amino acids in an amphitropic enzyme, CTP:phosphocholine cytidylyltransferase, dictate its selectivity for anionic membranes, *J. Biol. Chem. 278*, 514−522.
67. Burack, W. R., Gadd, M. E., and Biltonen, R. L. (1995) Modulation of phospholipase A2: identification of an inactive membrane-bound state, *Biochemistry 34*, 14819−14828.
68. Ghomashchi, F., Yu, B. Z., Berg, O., Jain, M. K., and Gelb, M. H. (1991) Interfacial catalysis by phospholipase A2: substrate specificity in vesicles, *Biochemistry 30*, 7318−7329.
69. Zhou, F., and Schulten, K. (1996) Molecular dynamics study of phospholipase A2 on a membrane surface, *Proteins 25*, 12−27.
70. Hyvonen, M. T., Oorni, K., Kovanen, P. T., and Ala-Korpela, M. (2001) Changes in a phospholipid bilayer induced by the hydrolysis of a phospholipase A2 enzyme: a molecular dynamics simulation study, *Biophys. J. 80*, 565−578.
71. Wooton-Kee, C. R., Boyanovsky, B. B., Nasser, M. S., de Villiers, W. J. S., and Webb, N. R. (2004) Group V sPLA(2) hydrolysis of low-density lipoprotein results in spontaneous particle aggregation and promotes macrophapge foam cell formation, *Arterioscler., Thromb., Vasc. Biol. 24*, 762−767.
72. Hakala, J. K., Oorni, K., Pentikaine, M. D., Hurt-Camejo, E., and Kovanen, P. T. (2001) Lipolysis of LDL by human secretory phospholipase A(2) induces particle fusion and enhances the retention of LDL to human aortic proteoglycans, *Arterioscler., Thromb., Vasc. Biol. 21*, 1053−1058.

BI051901T